

Ultrasound assessment of sheep stifle joint undergone lipopolysaccharide-induced synovitis

Ultrassonografia da articulação femorotibiopatelar em ovinos submetidos à indução de sinovite por lipopolissacarídeos

Michel Felipe Soares Souza¹ , Naida Cristina Borges¹ , Isabela Plaza Bittar¹ , Carla Amorim Neves¹ , Wanessa Patrícia Rodrigues da Silva^{1*} , Leandro Guimarães Franco¹ , Marco Augusto Machado Silva¹ 

¹Universidade Federal de Goiás (UFG), Goiânia, Goiás, Brazil.

*Correspondent: wrodrigues.vet@gmail.com

Abstract

Synovitis can be induced in animals through the application of bacterial wall lipopolysaccharide, and shows signs similar to naturally caused synovitis. Several studies have been carried out using the sheep species as an experimental model to understand osteoarticular diseases of the femorotibiopatellar joint in humans. There are echographic studies regarding the standardization of the femorotibiopatellar joint normality in sheep. However, for alterations such as acute synovitis, there is a gap in the literature. The objective was to serially describe the ultrasonographic aspects of the synovitis process induced by intra-articular infiltration of lipopolysaccharide from *Escherichia coli* (*E. coli*) in the femorotibiopatellar joint in sheep. Twelve healthy crossbred sheep (Santa Inês x Dorper) were used. Synovitis induction was performed only in the right FTP joints, which were evaluated by serial ultrasound examination at baseline (M0) and at 12 (M12), 24 (M24), 48 (M48), 72 (M72) and 120 (M120) hours after infiltration with lipopolysaccharide for the induction of synovitis. The intra-articular application of lipopolysaccharide from *E. coli* resulted in one or more sonographic signs of synovitis (increased volume of synovial fluid, pleating of the synovial membrane and cellularity in the joint cavity), which were identified early, 12 hours after inoculation, and regressed along the evaluated times ($p=0.0001$), until disappearing after 120 hours of inoculation.

Keywords: Arthritis; Lameness; Ultrasound; Stifle joint; Synovitis.

Resumo

A sinovite pode ser induzida em animais por meio da aplicação de lipopolissacarídeo de parede bacteriana, e apresenta sinais semelhantes à sinovite causada de forma natural. Diversos estudos têm sido realizados utilizando a espécie ovina como modelo experimental na compreensão das enfermidades osteoarticulares da articulação femorotibiopatelar (FTP) em humanos. Existem estudos ecográficos quanto a padronização da normalidade da articulação femorotibiopatelar em ovinos. Porém, para as alterações, como a sinovite aguda há lacuna na literatura. Objetivou-se descrever, de forma seriada, os aspectos ultrassonográficos do processo de sinovite induzida por infiltração intra-articular de lipopolissacarídeo de *Escherichia coli* (*E. coli*) na articulação femorotibiopatelar de ovinos. Foram utilizados 12 ovinos mestiços (Santa Inês x Dorper), hípidos. A indução da sinovite foi realizada apenas nas articulações FTP direitas, as quais foram avaliadas, por meio do exame ultrassonográfico de forma seriada, nos momentos basal (M0) e às 12 (M12), 24 (M24), 48 (M48), 72 (M72) e 120 (M120) horas após a infiltração com lipopolissacarídeo para a indução de sinovite. A aplicação intra-articular de lipopolissacarídeo de *E. coli* resultou em um ou mais sinais ecográficos de sinovite (aumento de volume do fluido sinovial, pregueamento da membrana sinovial e celularidade na cavidade articular), os quais foram identificados precocemente, 12 horas após a inoculação, e regrediram ao longo dos tempos avaliados ($p=0,0001$), até desaparecerem após 120 horas da inoculação.

Palavras-chave: Artrite; Claudicação; Joelho; Ultrassom; Sinovite.

Received: October 20, 2021. Accepted: January 12, 2022. Published: March 25, 2022.
www.revistas.ufg.br/vet visit the website to get the how to cite in the article page.

Introduction

The term synovitis refers to inflammation of the synovium, which aids in the nutrition of chondrocytes. Synovitis plays an important role in the development of arthritis, polyarthritis, or osteoarthritis, leading to cartilage destruction and synovial fibrosis.⁽¹⁾ It is a disease of great economic impact in sheep, as it results in lameness, joint stiffness, and reluctance to move.⁽²⁾

Ultrasonography is more sensitive than clinical

examination in detecting synovitis, as the animal may only present lameness in more advanced stages of the disease. Changes in echogenicity and echotexture in the synovium, in addition to an increase in synovial fluid, can be detected by this examination, which may be related to other findings indicative of arthritis/osteoarthritis.⁽³⁾

Experimentally, synovitis can be induced in animals^(1,4,5) through the application of recombinant equine interleukin-1 beta⁽⁶⁾ and bacterial wall lipopolysaccharide,^(1,5,7) and it shows signs similar to

naturally-occurring synovitis.^(1,4-8) The sheep species has been used over the years as one of the main experimental models for understanding osteoarticular diseases of the femorotibiopatellar joint in humans.⁽⁹⁻¹²⁾

However, there is a gap in the literature regarding the standardization of the ultrasound image of acute synovitis and the identification of elements in this joint in sheep. Some echographic studies have shown a normal pattern, with a detailed assessment of all the structures of this joint, which supports the studies of the diseases.⁽¹³⁻¹⁶⁾

This study aimed to serially describe the sonographic aspects of the synovitis process induced by intra-articular infiltration of *Escherichia coli* (*E. coli*) lipopolysaccharide in the femorotibiopatellar joint of sheep.

Material and methods

The present study was conducted with approval by the Animal Ethics Committee of the host institution (CEUA/UFG, protocol No. 063/16) and was associated with a study on pain in the femorotibiopatellar joint (FTP) caused by experimentally-induced synovitis.

Animals

Twelve crossbred sheep (Santa Inês x Dorper) aged between 9 and 12 months, weighing 38.9 ± 5.9 kg, were used. Inclusion criteria consisted of attesting the absence of clinical-orthopedic and ultrasound changes and complementary examinations, namely: blood count, total protein and fractions, creatinine, and GGT, which were within the parameters of normality for the species. Radiographic examination was not performed due to its low sensitivity and specificity compared to ultrasound examination for soft tissue changes.

All animals underwent a thirty-day adaptation with a vaccination protocol (Heptavac P Plus, MSD Animal Health, São Paulo, Brazil; 2 mL) and ecto-and endoparasite control. The sheep remained in two paddocks of 600 m², six in each, with masonry yards for resting, being supplemented with mineral salt, hay, and concentrate. Water was provided ad libitum in artificial drinking troughs.

Experimental design

Synovitis induction was performed only in the right FTP joints to allow restraint of the animals in right lateral recumbency, minimizing complications.

The animals were serially sedated with 0.1mg/kg of 2% xylazine intravenously (Xilasin[®], Syntec, Santana de Parnaíba, SP, Brazil) and placed in the right lateral decubitus position. After shaving and local antisepsis, a 24G catheter was introduced medially to the patellar ligament at the midpoint between its origin and

insertion, with the right FTP joint in maximum flexion and guided by ultrasound. Subsequently, intra-articular infiltration was performed according to the paraligamentous arthrocentesis technique described by Vandeweerd *et al.*,⁽¹⁷⁾ using 0.3 mL of phosphate buffer solution (PBS) containing 0.5 µg of *Escherichia coli* O55:B5 wall lipopolysaccharide extract (LPS L2880, Sigma, St. Louis, MO, USA).⁽³¹⁾ This synovitis induction protocol was standardized using the technique described by Bittar *et al.*⁽³¹⁾

The right FTP joints were evaluated serially by ultrasound examinations in two-dimensional mode (Mode B) at baseline moment (M0) and 12 (M12), 24 (M24), 48 (M48), 72 (M72), and 120 (M120) hours after infiltration with lipopolysaccharide for synovitis induction. Ultrasound images of the limb at baseline (M0) were considered as a negative control.

Ultrasound examination

Examination in Mode B of the right FTP joint was performed using a Logiq-E[®] device (G&E, São Paulo, SP, Brazil) coupled to a multifrequency linear transducer (7.5–10 MHz) at a frequency of 10 MHz. Then, an extensive shaving of the FTP region was performed from the proximal third of the thigh to the distal third of the leg with an Oster[®] device (Oster, São Paulo, SP, Brazil) and a #40 blade. Ultrasound gel was applied at the time of examination for better contact between the skin and the transducer.

Scans were performed following the instructions of Vandeweerd *et al.*⁽¹⁷⁾ and Kramer *et al.*,⁽¹⁸⁾ with transducer positioning in longitudinal and sagittal planes to the lateral and medial accesses, between the femoral condyles, patella and condyles and tibial tuberosity, considering the joint space on the dorsal, lateral, and medial face as anatomic landmarks to visualize recesses, compartments, tendons, ligaments, bone surfaces, and muscles.

Joint cavities and compartments were evaluated for changes in synovial fluid volume, folding of the synovial membrane, and presence/absence of cellularity in the synovial fluid.⁽³⁾ Bone structures were evaluated for bone surface contour and echogenicity. Echogenicity and the presence/absence of irregularities in the edges of the growth plates were also observed. Muscles, tendons, and ligaments were evaluated for echogenicity and echotexture.^(16,18)

Statistical analysis

Friedman's and Dunn's post-hoc tests were used for pairwise comparison (M0 x M12 to 120) of qualitative variables (increased size of the joint cavity, folding of the synovial membrane, and cellularity in the joint cavity).

The software Graphpad Prism 5 was used for the analyses. The significance level for all tests was 5%.

Results

Intra-articular application of *E. coli*

lipopolysaccharide resulted in one or more echographic signs of synovitis (increased synovial fluid volume, folding of the synovial membrane, and cellularity in the joint cavity), which were identified early, i.e., 12 hours after inoculation, and regressed over the evaluated times (Figures 1, 2, and 3) ($p=0.0001$) until they disappeared 120 hours after inoculation (Table 1).

Table 1. Absolute number and frequency (%) of statistically significant sonographic changes observed by comparing baseline (M0) and 12 (M20), 24 (M24), 48 (M48), 72 (M72), and 120 (M120) after synovitis induction in the femorotibiopatellar joint of young sheep. The value zero (0) means that the change at a certain time was statistically insignificant

| Ultrasound access | Ultrasound change | Moment | | | | |
|---------------------------------|----------------------------------|-----------|-----------|------------|-----------|-----------|
| | | M0 x M12 | M0 x M24 | M0 x M48 | M0 x M72 | M0 x M120 |
| Lateral | | | | | | |
| Femorotibiopatellar compartment | Increased synovial fluid volume | 12 (100) | 11 (91.7) | 11 (91.7) | 0 (0) | 0 (0) |
| | Folding of the synovial membrane | 11 (91.7) | 8 (66.7) | 8 (66.7) | 8 (66.7) | 0 (0) |
| Tendinous recess | Increased synovial fluid volume | 0 (0) | 11 (91.7) | 11 (91.7) | 0 (0) | 0 (0) |
| | Cellularity in the joint cavity | 0 (0) | 0 (0) | 9 (75.0) | 0 (0) | 0 (0) |
| Medial | | | | | | |
| Femorotibiopatellar compartment | Increased synovial fluid volume | 12 (100) | 10 (83.3) | 10 (83.3) | 10 (83.3) | 0 (0) |
| | Increased synovial fluid volume | 12 (100) | 12 (100) | 10 (83.34) | 0 (0) | 0 (0) |
| Supracondylar recess | Folding of the synovial membrane | 10 (83.3) | 0 (0) | 0 (0) | 0 (0) | 0 (0) |
| | Cellularity in the joint cavity | 9 (75.0) | 0 (0) | 0 (0) | 0 (0) | 0 (0) |

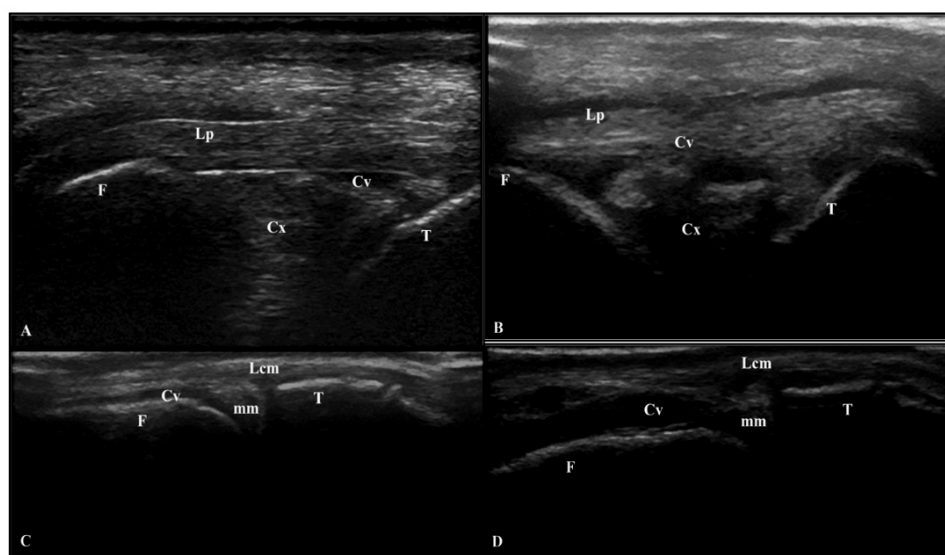


Figure 1. Longitudinal ultrasound images of the femorotibiopatellar joint of a sheep at moments M0, before performing lipopolysaccharide infiltration for induction of synovitis, and M24, after induction, with an increase in the synovial fluid volume. A: infrapatellar region at moment M0. F. femur; T. tibia; Lp. patellar ligament; Cx. infrapatellar fat pad; Cv. joint cavity – cranial portion of the femorotibial compartment. B: infrapatellar region at moment M24. A moderate amount of anechogenic content is observed adjacent to the infrapatellar fat pad, indicating synovial effusion. F. femur; T. tibia; Lp. patellar ligament; Cx. infrapatellar fat pad; Cv. joint cavity – cranial portion of the femorotibial compartment. C: medial femorotibial compartment at moment M0. F. femur; T. tibia; Lcm. medial collateral ligament; mm. medial meniscus; Cv. joint cavity – medial portion of the medial femorotibial compartment. D: medial region at moment M24. Moderate amount of anechogenic content between the medial collateral ligament and the femur, indicating synovial effusion. F. femur; T. tibia; Lcm. medial collateral ligament; mm. medial meniscus; Cv. joint cavity – medial portion of the medial femorotibial compartment.

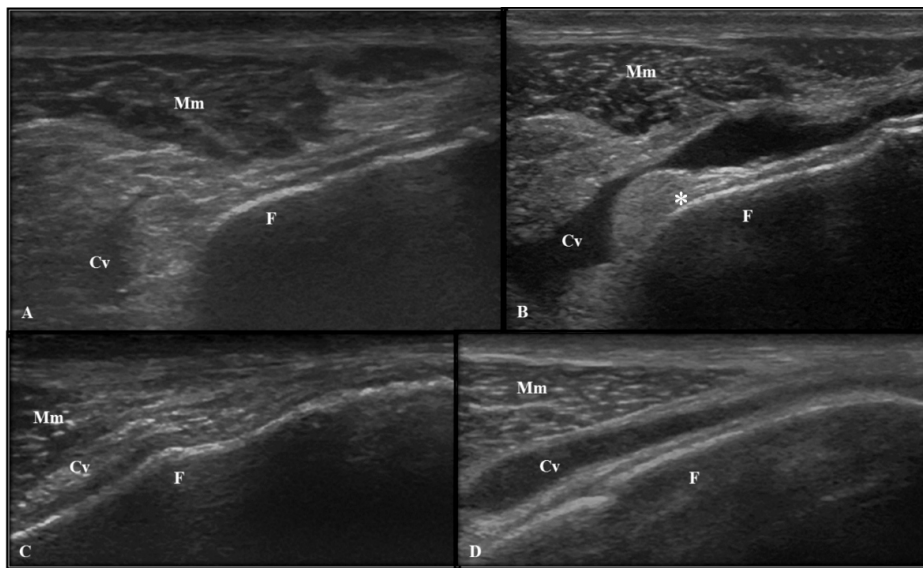


Figure 2. Longitudinal ultrasound images of the femorotibiopatellar joint of a sheep at moments M0, before performing lipopolysaccharide infiltration for induction of synovitis, and M12 and M24, after induction, with an increase in synovial fluid volume (B and D) and thickening of the synovial membrane (B). A: region of the lateral portion of the femoropatellar compartment at moment M0. F. femur; Mm. muscle belly of the vastus lateralis muscle; Cv. joint cavity – lateral portion of the femoropatellar compartment. B: region of the lateral portion of the femoropatellar compartment at moment M12. Joint cavity edges distended due to increased synovial fluid, with thickening of the synovial membrane. The presence of a hypoechoic proliferative tissue (asterisk) is another sign of this change. F. femur; Mm. muscle belly of the vastus lateralis muscle; Cv. joint cavity – lateral portion of the femoropatellar compartment. C: region of the medial portion of the femoropatellar compartment at moment M0. F. femur; Mm. muscle belly of the vastus medialis muscle; Cv. joint cavity – medial portion of the femoropatellar compartment. D: region of the medial portion of the femoropatellar compartment at moment M24. There was an increase in synovial fluid in the joint cavity. F. femur; Mm. muscle belly of the vastus medialis muscle; Cv. joint cavity – medial portion of the femoropatellar compartment.

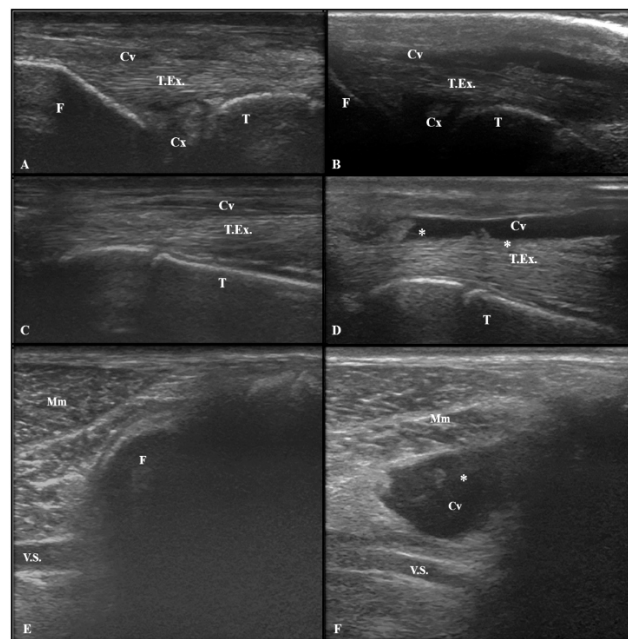


Figure 3. Longitudinal ultrasound images of the femorotibiopatellar joint of a sheep at moments M0, before performing lipopolysaccharide infiltration for induction of synovitis, and M24 and M48, after induction, with an increase in synovial fluid volume and thickening and proliferation of the synovial membrane. A: craniolateral region at moment M0. F. femur; T. tibia; T.Ex. tendon originating from the femur in common of the fibularis tertius, extensor digitorum longus, and extensor digitorum III muscles; Cx. infrapatellar fat pad; Cv. joint cavity – craniolateral portion of the femorotibial compartment. B: craniolateral region at moment M48. F. femur; T. tibia; T.Ex. tendon originating from the femur in common of the fibularis tertius, extensor digitorum longus, and extensor digitorum III muscles; Cx. infrapatellar fat pad; Cv. joint cavity – craniolateral portion of the femorotibial compartment. C: tendon sheath originating from the extensor muscles at moment M0. T. tibia; T.Ex. tendon originating from the femur in common of the fibularis tertius, extensor digitorum longus, and extensor digitorum III muscles; Cv. joint cavity – tendinous recess. D: tendon sheath originating from the extensor muscles at moment M24. Irregular and hypoechoic proliferative tissue, characteristic of thickening and proliferation of the synovial membrane (asterisks) is observed inside the joint cavity with increased synovial fluid volume. T. tibia; T.Ex. tendon originating from the femur in common of the fibularis tertius, extensor digitorum longus, and extensor digitorum III muscles; Cv. joint cavity – tendinous recess. E: medial supracondylar recess at moment M0. F. femur; Mm. muscle belly of the semimembranosus and gracilis muscles; V.S. medial saphenous vein. F: medial supracondylar recess at moment M24. Irregular edges and the presence of hypoechoic material within the joint cavity (asterisk) indicate thickening and proliferation of the synovial membrane. F. femur; Mm. muscle belly of the semimembranosus and gracilis muscles; V.S. medial saphenous vein. Cv. joint cavity – medial supracondylar recess.

Discussion

Distension, with a consequent increase in joint volume, was one of the main echographic changes found in this study involving lipopolysaccharide-induced synovitis, using the sheep species as an experimental model. Joint effusion in seven out of the nine echographic accesses was observed as an increase in the synovial fluid volume in at least one of the moments after inoculation. This was the most observed change relative to the incidence of observed animals and the number of affected regions. Joint effusion was evaluated in the suprapatellar echographic position in human patients, described as mobile anechoic or hypoechoic intra-articular content, which deforms under local compression.⁽¹⁹⁾ Horses with meniscal injury showed a high frequency in the medial femorotibial compartment and a low frequency in the lateral femorotibial compartment. The femoropatellar compartment was also evaluated, but no changes related to synovitis were observed, different from what was observed in humans.⁽²⁰⁾ The present study shows changes that are similar to those observed in humans, as the increase in volume was the most incident both in the lateral and medial portions of the femoropatellar compartment.

The synovial fluid volume in the femorotibiopatellar joint of sheep varies from 0.67 to 1.19 mL, with a mean of 0.93 mL.⁽²¹⁾ The lipopolysaccharide solution volume used for synovitis induction in this study was 0.3 mL. This amount was not enough to cause the distention found in the ultrasound accesses. A study carried out with the sheep species required the administration of 10 mL of meglumine and sodium ioxaglate solution to obtain minimum back pressure inside the joint, indicating its maximum volumetric capacity.⁽¹⁷⁾ A post-mortem study to determine echographic accesses of this joint in sheep used 20 mL of saline solution to obtain an expansion of the joint cavity.⁽¹⁶⁾ Therefore, in the present study, the increased synovial fluid volume was believed to be mediated by inflammation and not by the injected volume.

The epithelial tissue of the synovial membrane is stimulated by tumor necrosis factor- α , interleukin-1, and interleukin-6 released by macrophages in the face of aggression, including the presence of lipopolysaccharide, which undergoes hyperplasia with monocytic and lymphocytic infiltrate in the subepithelial layer. Macroscopically, a diffuse thickening is observed in the synovial membrane, associated with nodule formation.⁽²¹⁻²⁴⁾ This macroscopic change was identified in this study as a folding of the synovial membrane on echographic examination. The echographic image of this change in this study was determined as the presence of an irregularly shaped hypoechoic structure that lines the joint cavity internally (folding) and without mobility within the

synovial fluid. These signs are consistent with what was observed in echographic images of joints in humans^(19,25) and horses⁽²⁰⁾ with synovitis.

Human synovial membrane hypertrophy was considered as an abnormal hypoechoic intra-articular tissue that is not detachable from the joint capsule and does not change its shape upon compression. This aspect was observed in the longitudinal echographic position of the suprapatellar pouch of the knee in humans with osteoarthritis.⁽¹⁹⁾ The site where this change was observed in humans is similar to that described in the present study for sheep (lateral segment of the femoropatellar compartment), both related to the femoropatellar compartment. Hull *et al.*⁽²⁵⁾ quantified the thickness of the synovial membrane observed in an echographic image using software that counts the number of pixels in a given area. An increase in the thickness of this structure has been observed in human patients with synovitis in the metacarpophalangeal joint caused by rheumatoid arthritis. The proliferation of the synovial membrane was also observed in the echographic study of the medial femorotibial compartment of horses with meniscal injury in a different location from the one observed in the present study.⁽²⁰⁾ Similar to what was found in humans,^(19,25) the proliferation of the synovial membrane was identified as a sign of synovitis in sheep using an echographic examination.

The cellularity in the joint cavity was described in the present experiment as hyperechoic points suspended in the synovial fluid and with mobility, without acoustic shadow formation. Similar signs could be observed in the medial femorotibial compartment of horses with meniscal injury.⁽²⁰⁾ This echographic aspect is compatible with fibrin particles, meniscal and cartilaginous debris released into the synovial fluid.⁽²⁶⁾ Cellularity is believed to be related, in the present study, to the presence of fibrin particles resulting from lipopolysaccharide-induced synovitis, as no change was observed in the echographic image of menisci and cartilage. The region where cellularity was identified in sheep (medial supracondylar recess and tendon recess) was different from that reported for other species.^(20,26) These recesses, which are absent or proportionately smaller in other species, are located far from joint surfaces, which causes a decrease in synovial fluid movement. The stasis of the synovial fluid is assumed to facilitate the sedimentation of debris, which increases the chance of their visualization.

The three signs suggestive of synovitis were possible to be identified from 12 hours after the induction of inflammation. It reinforces the importance of joint echographic examination, especially for the detection of lesions in their initial phases. However, there is a need for evaluations before the time of 12 hours to classify the detection of changes as early. On the other hand, the radiographic examination of the same joint is capable of

identifying lesions related to chronic diseases, such as osteochondrosis⁽²⁷⁾ and osteophytosis.⁽²⁸⁾

The joint echographic examination can also detect bone lesions that are a consequence of joint inflammation. The sonographic image of erosion of the subchondral bone is defined by Kaeley *et al.*⁽³⁾ as the intra-articular discontinuity of the bone surface. Osteophytosis is seen by calcification within tendons and their thickening. In humans, these lesions are a consequence of prolonged joint inflammation. Therefore, they were reported as frequent in chronic conditions. In this case, as the synovitis was induced by LPS and regressed within a few hours, there was no time for a chronic lesion to set in. This is the reason why no signs of bone erosion were observed in the animals in this experiment.

An important aspect of the present study was the establishment of the sheep species as an experimental model for echographic evaluation of the femorotibiopatellar joint in synovitis. Kayser *et al.*⁽¹⁶⁾ described the echographic accesses for the evaluation of several constituents of this joint in sheep. All accesses described in this study are consistent with previously described accesses,⁽¹⁶⁾ except for the medial supracondylar recess, which could not be visualized by them. There is a need for a more detailed investigation into why this recess is seen in an *in vivo* model of synovitis and is not seen in a post-mortem fluid volume infusion model. Another difference is that transverse accesses were not evaluated in this study, which may have impaired the visualization of expansions in recesses.

The sheep species is easily physically restrained, with a docile behavior, and the stifle joint is the one that most resembles the knee joint of the human species for studies of osteoarticular diseases and surgical techniques compared to other species.^(29,30) Furthermore, in the authors' opinion, it has ideal joint dimensions for performing ultrasound examinations.⁽³¹⁾ The optimization and reduction in the number of animals submitted to stressful experimental situations constitutes one of the ethical principles of its use in experimentation.⁽³²⁾

The limitations of this study are related to the scarcity of reports and the establishment of a parallel between synovitis and joint echographic examination in sheep, which limited the standardization of procedures. Four out of nine used echographic accesses were adapted from a study with dogs.⁽¹⁸⁾ The other positions were explored during the preliminary phase of the experiment, based on an article on contrast examination of computed tomography and radiography of the femorotibiopatellar joint cavity in sheep.⁽¹⁷⁾ The joint echographic examination is difficult to perform and interpret. Therefore, exhaustive training of the evaluator was necessary to perform the experimental procedures.

Conclusion

Ultrasonography of the femorotibiopatellar joint in sheep was effective in detecting synovitis experimentally induced by intra-articular infiltration of *E. coli* lipopolysaccharide. The most common sign related to synovitis was the increased joint cavity volume, followed by folding of the synovial membrane and cellularity in the joint cavity, predominantly observed at 12, 24, and 48 hours after infiltration.

Conflict of interest

The authors declare no conflicts of interest.

Authors contribution

Conceptualization: M. F. S. Souza, C. A. Neves, I. P. Bittar, N. C. Borges, L. G. Franco, M. A. M. Silva; *Formal Analysis:* M. F. S. Souza; *Investigation:* M. F. S. Souza, C. A. Neves, I. P. Bittar, W. P. R. Silva; *Methodology:* M. F. S. Souza, I. P. Bittar, N. C. Borges, L. G. Franco, M. A. M. Silva; *Project administration:* M. F. S. Souza, C. A. Neves, I. P. Bittar, W. P. R. Silva, N. C. Borges, L. G. Franco, M. A. M. Silva; *Resources:* I. P. Bittar, N. C. Borges; *Supervision:* N. C. Borges, L. G. Franco, M. A. M. Silva; *Validation:* M. F. S. Souza, C. A. Neves, I. P. Bittar, W. P. R. Silva, N. C. Borges, L. G. Franco, M. A. M. Silva; *Visualization:* M. F. S. Souza, N. C. Borges; *Writing (original draft):* M. F. S. Souza, N. C. Borges; *Writing (review & editing):* M. F. S. Souza, I. P. Bittar, W. P. R. Silva, N. C. Borges.

References

- Otterness IG, Bliven ML, Milici AJ, Poole AR. Comparison of mobility changes with histological and biochemical changes during lipopolysaccharide-induced arthritis in the hamster. *The American Journal of Pathology* [internet]. 1994 Mai [cited 2021 Oct. 10];144(5):1098. Available on: <https://pubmed.ncbi.nlm.nih.gov/8178933>.
- Abdalmula A, Washington EA, House JV, Dooley LM, Blacklaws BA, Ghosh P, Bailey SR, Kimpton WG. Clinical and histopathological characterization of a large animal (ovine) model of collagen-induced arthritis. *Veterinary Immunology and Immunopathology* [internet]. 2014 May [cited 2021 Oct. 10];15;159(2):83-90. Available on: <https://pubmed.ncbi.nlm.nih.gov/24703062>.
- Kaeley GS, Bakewell C, Deodhar A. The importance of ultrasound in identifying and differentiating patients with early inflammatory arthritis: a narrative review. *Arthritis Research & Therapy* [internet]. 2020 Dez [cited 2021 Oct. 10];22(1):1-0. Available on: <https://doi.org/10.1186/s13075-019-2050-4>.
- Miyazaki S, Matsukawa A, Ohkawara S, Takagi K, Yoshinaga M. Neutrophil infiltration as a crucial step for monocyte chemoattractant protein (MCP)-1 to attract monocytes in lipopolysaccharide-induced arthritis in rabbits. *Inflammation Research* [internet]. 2000 Dez [cited 2021 Oct. 10];49(12):673-8. Available on: <https://doi.org/10.1007/s000110050645>.

5. Tanaka D, Kagari T, Doi H, Shimozato T. Essential role of neutrophils in anti-type II collagen antibody and lipopolysaccharide-induced arthritis. *Immunology* [internet]. 2006 Oct. [cited 2021 Oct. 10];119(2):195-202. Available on: <https://doi.org/10.1111/j.1365-2567.2006.02424.x>.
6. Watkins A, Fasanello D, Stefanovski D, Schurer S, Caracappa K, D'Agostino A, Costello E, Freer H, Rollins A, Read C, Su J. Investigation of synovial fluid lubricants and inflammatory cytokines in the horse: a comparison of recombinant equine interleukin 1 beta-induced synovitis and joint lavage models. *BMC Veterinary Research* [internet]. 2021 Dez [cited 2021 Oct. 10];17(1):1-8. Available on: <https://doi.org/10.1186/s12917-021-02873-2>.
7. Park MH, Yoon DY, Ban JO, Kim DH, Lee DH, Song S, Kim Y, Han SB, Lee HP, Hong JT. Decreased severity of collagen antibody and lipopolysaccharide-induced arthritis in human IL-32 β overexpressed transgenic mice. *Oncotarget* [internet]. 2015 Nov [cited 2021 Oct. 10];17;6(36):385-96. Available on: <https://doi.org/10.18632/oncotarget.6160>.
8. Oliveira DP, Augusto GG, Batista NV, de Oliveira VL, Ferreira DS, e Souza MA, Fernandes C, Amaral FA, Teixeira MM, de Padua RM, Oliveira MC. Encapsulation of trans-aconitic acid in mucoadhesive microspheres prolongs the anti-inflammatory effect in LPS-induced acute arthritis. *European Journal of Pharmaceutical Sciences* [internet]. 2018 Jul [cited 2021 Oct. 10];119:112-20. Available on: <https://doi.org/10.1016/j.ejps.2018.04.010>.
9. Orth P, Meyer HL, Goebel L, Eldracher M, Ong MF, Cucchiari M, Madry H. Improved repair of chondral and osteochondral defects in the ovine trochlea compared with the medial condyle. *Journal of Orthopaedic Research* [internet]. 2013 Nov [cited 2021 Oct. 10];31(11):1772-9. Available on: <https://doi.org/10.1002/jor.22418>.
10. Zorzi AR, Amstalden EM, Plepis AM, Martins VC, Ferretti M, Antonioli E, Duarte AS, Luzo A, Miranda JB. Effect of human adipose tissue mesenchymal stem cells on the regeneration of ovine articular cartilage. *International Journal of Molecular Sciences* [internet]. 2015 Nov [cited 2021 Oct. 10];16(11):26813-31. Available on: <http://doi.org/10.3390/ijms161125989>.
11. Risch M, Easley JT, McCready EG, Troyer KL, Johnson JW, Gadowski BC, McGilvray KC, Kisiday JD, Nelson BB. Mechanical, biochemical, and morphological topography of ovine knee cartilage. *Journal of Orthopaedic Research* [internet]. 2021 Abr [cited 2021 Oct. 10];39(4):780-7. Available on: <https://doi.org/10.1002/jor.24835>.
12. Bellrichard M, Snider C, Kuroki K, Brockman J, Grant DA, Grant SA. The use of gold nanoparticles in improving ACL graft performance in an ovine model. *Journal of Biomaterials Applications* [internet]. 2021 Set [cited 2021 Oct. 10];1-11. Available on: <https://doi.org/10.1177/08853282211039179>.
13. Macrae AI, Scott PR. The normal ultrasonographic appearance of ovine joints, and the uses of arthrosonography in the evaluation of chronic ovine joint disease. *The Veterinary Journal* [internet]. 1999 Set [cited 2021 Oct. 10];158(2):135-43. Available on: <https://doi.org/10.1053/tvjl.1998.0353>.
14. Hette K, Rahal SC, Mamprim MJ, Volpi RD, Silva VC, Ferreira DO. Avaliações radiográfica e ultra-sonográfica do joelho de ovinos. *Pesquisa Veterinária Brasileira* [internet]. 2008 [cited 2021 Oct. 10];28:393-8. Available on: <https://doi.org/10.1590/S0100-736X2008000900001>.
15. Sideri A, Tsioli V. Ultrasonographic examination of the musculoskeletal system in sheep. *Small Ruminant Research* [internet]. 2017 Jul [cited 2021 Oct. 10];152:158-61. Available on: <https://doi.org/10.1016/j.smallrumres.2016.12.018>.
16. Kayser F, Hontoir F, Clegg P, Kirschvink N, Dugdale A, Vandeweerd JM. Ultrasound anatomy of the normal stifle in the sheep. *Anatomia, Histologia, Embryologia* [internet]. 2019 Jan [cited Oct. 10];48(1):87-96. Available on: <https://doi.org/10.1111/ahc.12414>.
17. Vandeweerd JM, Kirschvink N, Muylkens B, Depiereux E, Clegg P, Herteman N, Lamberts M, Bonnet P, Nisolle JF. A study of the anatomy and injection techniques of the ovine stifle by positive contrast arthrography, computed tomography arthrography and gross anatomical dissection. *The Veterinary Journal* [internet]. 2012 Ago [cited 2021 Oct. 10];193(2):426-32. Available on: <https://doi.org/10.1016/j.tvjl.2011.12.011>.
18. Kramer M, Stengel H, Gerwing M, Schimke E, Sheppard C. Sonography of the canine stifle. *Veterinary Radiology & Ultrasound* [internet]. 1999 Mai [cited 2021 Oct. 10];40(3):282-93. Available on: <https://doi.org/10.1111/j.1740-8261.1999.tb00363.x>.
19. Bevers K, Bijlsma JW, Vriezckolk JE, van den Ende CH, den Broeder AA. Ultrasonographic features in symptomatic osteoarthritis of the knee and relation with pain. *Rheumatology* [internet]. 2014 Set [cited 2021 Oct. 10];53(9):1625-9. Available on: <https://doi.org/10.1093/rheumatology/keu030>.
20. De Busscher V, Verwilghen D, Bolen G, Serteyn D, Busoni V. Meniscal damage diagnosed by ultrasonography in horses: a retrospective study of 74 femorotibial joint ultrasonographic examinations (2000–2005). *Journal of Equine Veterinary Science* [internet]. 2006 Oct. [cited 2021 Oct. 10];26(10):453-61. Available on: <https://doi.org/10.1016/j.jevs.2006.08.003>.
21. Vandeweerd JM, Hontoir F, Kirschvink N, Clegg P, Nisolle JF, Antoine N, Gustin P. Prevalence of naturally occurring cartilage defects in the ovine knee. *Osteoarthritis and Cartilage* [internet]. 2013 Ago [cited 2021 Oct. 10];21(8):1125-31. Available on: <https://doi.org/10.1016/j.joca.2013.05.006>.
22. Botez P, Sirbu PD, Grierosu C, Mihailescu D, Savin L, Scarlat MM. Adult multifocal pigmented villonodular synovitis—clinical review. *International Orthopaedics* [internet]. 2013 Abr [cited 2021 Oct. 10];37(4):729-33. Available on: <https://doi.org/10.1007/s00264-013-1789-5>.
23. Grauw JC, Van de Lest CH, Brama PA, Rambags BP, Van Weeren PR. In vivo effects of meloxicam on inflammatory mediators, MMP activity and cartilage biomarkers in equine joints with acute synovitis. *Equine veterinary journal*. 2009 Set [cited 2021 Oct. 10];41(7):693-9. Available on: <https://doi.org/10.2746/042516409X436286>.
24. Hayashi D, Roemer FW, Katur A, Felson DT, Yang SO, Alomran F, Guermazi A. Imaging of synovitis in osteoarthritis: current status and Oct.look. *Seminars in arthritis and rheumatism* [internet]. 2011 Oct. [cited 2021 Oct. 10];41(2):116-130. Available on: <https://doi.org/10.1016/j.semarthrit.2010.12.003>.
25. Hull DN, Cooksley H, Chokshi S, Williams RO, Abraham S, Taylor PC. Increase in circulating Th17 cells during anti-TNF therapy is associated with ultrasonographic improvement of synovitis in rheumatoid arthritis. *Arthritis research & therapy* [internet]. 2016 Dez [cited 2021 Oct. 10];18(1):1-2. Available on: <https://doi.org/10.1186/s13075-016-1197-5>.
26. Denoix JM, Audigie F. Ultrasonographic examination of the stifle in horses. *Proceedings of the 13th ACVS Veterinary Symposium*. Washington, DC, USA. Bethesda, MD: American

College of Veterinary Surgeons 2003 [cited Oct. 10];219–222. Available on: <https://hal.inrae.fr/hal-02825933>.

27. Beccati F, Chalmers HJ, Dante S, Lotto E, Pepe M. Diagnostic sensitivity and interobserver agreement of radiography and ultrasonography for detecting trochlear ridge osteochondrosis lesions in the equine stifle. *Veterinary Radiology & Ultrasound* [internet]. 2013 Mar [cited 2021 Oct. 10];54(2):176-84. Available on: <https://onlinelibrary.wiley.com/doi/abs/10.1111/vru.12004>.

28. Lasalle J, Alexander K, Olive J, Laverty S. Comparisons among radiography, ultrasonography and computed tomography for ex vivo characterization of stifle osteoarthritis in the horse. *Veterinary Radiology & Ultrasound* [internet]. 2016 Set [cited 2021 Oct. 2021];57(5):489-501. Available on: <https://doi.org/10.1111/vru.12370>.

29. Osterhoff G, Löffler S, Steinke H, Feja C, Josten C, Hepp P. Comparative anatomical measurements of osseous structures in the ovine and human knee. *The Knee* [internet]. 2011 Mar [cited

2021 Oct. 10];18(2):98-103. Available on: <https://doi.org/10.1016/j.knee.2010.02.001>.

30. Proffen BL, McElfresh M, Fleming BC, Murray MM. A comparative anatomical study of the human knee and six animal species. *The Knee* [internet]. 2012 Ago [cited 2021 Oct. 10];19(4):493-9. Available on: <https://doi.org/10.1016/j.knee.2011.07.005>.

31. Bittar IP, Neves CA, Araújo CT, Oliveira YV, Silva SL, Borges NC, Franco LG. Dose-Finding in the Development of an LPS-Induced Model of Synovitis in Sheep. *Comparative Medicine* [internet]. 2021 Abr [cited 2021 Oct. 10];71(2):141-7. Available on: <https://doi.org/10.30802/aalas-cm-20-000032>

32. Ministério da Ciência, Tecnologia e Inovação Conselho Nacional de Controle de Experimentação Animal – CONCEA. Diretriz Brasileira Para o Cuidado e a Utilização de Animais Para Fins Científicos e Didáticos – DBCA. Brasília: 2013. 50p. Brasil.